SUPPLEMENTAL MATERIAL

Class I Histone Deacetylase Inhibition for the Treatment of Sustained Atrial Fibrillation

Mitsuru Seki, Ryan LaCanna, Jeffery Powers, Christine Varkas, , Fang Liu, Remus Berretta, Geena Chacko, John Holten, Pooja Jadiya, Tao Wang, Jeffery S. Arkles, Joshua M. Cooper, Steven R. Houser, Jianhe Huang, Vickas V. Patel, Fabio A. Recchia

The Journal of Pharmacology and Experimental Therapeutics

Expanded Methods

Pacemaker implantation in dogs

At least 10 days after the dogs recovered from the open thoracotomy, we implanted a single-chamber atrial pacemaker in ten dogs. The dogs were intubated and anesthetized as described in the main text, and then a cut-down was performed to isolate the right internal jugular vein. The jugular vein was accessed using the modified Seldinger technique and a splitable, hemostatic sheath was passed into the vein. Under fluoroscopic guidance, an active fixation pacing lead (5077, Medtronic Inc.) was positioned on the posterior right atrial wall. When good sensing with a pacing threshold <0.5V @ 0.5ms was obtained, the lead was fixed on the posterior atrial wall by deploying the helix. The sheath was removed, the lead was tied down to the underlying muscle and tunneled to a subcutaneous pocket fashioned on the posterior aspect of the animal's neck. The lead was then placed into the ventricular pacing port of a biventricular pacemaker (Consulta CRT-P, Medtronic Inc.) and the atrial and left ventricular pacing ports were plugged. The pacemaker was then placed in the subcutaneous pocket, flushed with saline and the incisions were closed in layers. The dogs were given antibiotics for the next three days, before starting the pacing protocol.

Transthoracic echocardiography

Protocols for murine (Liu et al., 2008; Yuan et al., 2010) and canine (Mitacchione et al., 2014; Woitek et al., 2015) transthoracic echocardiography have been previously described. Briefly, 16 *Hopx*^{Tg} (8 treated with CI994 and 8 treated with vehicle) and 16 wild-type littermate control mice (8 treated with CI994 and 8 treated with vehicle) were anesthetized with 0.75-1% isoflourane plus 100% oxygen while supine on a heated platform. An additional infrared heating lamp was used to maintain body temperature at 37±0.5°C throughout the procedure. An ECG signal was obtained from the electrode pads on the heated platform, and chest hairs were removed using a chemical depilator (Nair) to minimize ultrasound attenuation. Dogs were not anesthetized and laid recumbent on a table for the procedure. Echocardiographic analysis was performed on a total of 15 dogs, 5 in sinus rhythm, 5 with atrial tachypacing-induced AF given vehicle and 5 with atrial tachypacing-induced AF treated with CI994. For the mice, transthoracic echocardiography was performed using a Vevo 770 VisualSonic machine (Toronto, Canada) equipped with a linear 30-MHz probe (RMV 707B) for mice. Two-dimensional images were recorded in the parasternal long- and short-axis projections to guide M-mode recordings obtained at the mid-ventricular level in both views. Digital images were obtained at a frame rate of 180 images/sec. Thickness of the left ventricule (LV) interventricular septum (IVS) and posterior wall (PW) were measured and the average value from both views reported. We computed LV fractional shortening, LVFS=(LVIDd-LVIDs)/LVIDd), and LV ejection fraction, LVEF=(LVIDd^3-LVIDs^3)/LVIDd^3, from the M-mode measurements. In the dogs an echocardiographic examination was performed at baseline and then weekly using an Esaote MyLab 30 CV echocardiography system (Esaote, Florence, Italy). Minimum views included the right parasternal short-axis, long axis as well as an apical four chamber and two chamber views of at least five consecutive cardiac cycles at a frame rate of 40.7 images/second. Ejection fraction was evaluated using the Simpson formula in the apical views. Chamber size and septal and lateral systolic wall thickening were obtained from M-Mode measurements.

Electrophysiology studies in mice

Surface ECG and invasive mouse electrophysiology studies were performed as previously described(Ismat et al., 2005; Li et al., 2005; Liu et al., 2008; Levin et al., 2009; Liu et al., 2015). Surface ECG recordings and complete in vivo electrophysiological studies (EPS) were obtained from eight *Hopx*^{Tg} mice treated with vehicle (5% DMSO) and eight *Hopx*^{Tg} mice treated with

CI994 (aged 14-17 weeks), as well as eight age-matched non-transgenic wild-type littermates treated with vehicle and eight age-matched non-transgenic wild-type littermates treated with CI994. Each mouse was anesthetized with 1.0-1.5% isoflourane plus 100% oxygen, and multi-lead ECGs were obtained using 26-gauge subcutaneous electrodes. Core body temperature was maintained with an infrared heating lamp at 33-34°C and monitored with a rectal probe. A jugular vein cutdown was performed and an octapolar 1.0-French electrode catheter (EP800, Millar Instruments Inc. Houston, TX) placed in the right atrium and ventricle under electrogram guidance to confirm catheter position. A programmed digital stimulator (DTU-215A, Bloom Associates Ltd., Reading, PA) was used to deliver electrical impulses at approximately twice the diastolic threshold. Surface ECG and intracardiac electrograms were simultaneously displayed on a multichannel oscilloscope recorder (Bard Electrophysiology, Inc. Lowell, MA) at a digitization rate of 2 kHz and stored on optical media for offline analysis. ECG channels were filtered from 0.5-250 Hz and intracardiac electrograms were filtered from 5-400 Hz. ECG intervals were measured by two independent observers blinded to the animal's genotype. We considered an arrhythmic episode to be the induction of three or more consecutive ectopic beats following the last extrastimuli of a drive train.

The *in vivo* study began by determining atrial and ventricular capture thresholds. We start with a capture output of 0.1 mA at 1.0 ms (with good catheter position capture threshold should be 0.1 mA or less) and then place the output at 0.2 mA or twice the diastolic threshold if capture threshold is between 0.1 - 0.2 mA. If capture threshold is above 0.2 mA, then the catheter position is readjusted until the capture threshold is acceptable. Sinus Node Recovery Times were determined by delivering atrial pacing at drive cycle lengths of 120 and 100 ms for 15 seconds each, and then measuring the recovery time to the first atrial electrogram from the last S1 of the train. AV Nodal Conduction was determined by delivering atrial pacing starting at 150 ms and decrement by 10 ms down to the AV Wenckebach cycle length. Then we increase the atrial pacing cycle length by 5 ms to see if there is either 1:1 conduction or Wenckebach. We continue delivering atrial burst pacing and decrement by 10 ms down to 2:1 conduction and then increase the atrial pacing cycle length by 5 ms to see if there is still 2:1 conduction or Wenckebach. AV Node Effective Refractory Period was determining by delivering a drive cycle of 120 ms with an S2 coupled at 115 ms and we then brought in S2 by 5 ms until there was no longer conduction to the ventricle. Atrial Effective Refractory Period was determined by beginning at a drive cycle of

120 ms with an S2 coupled at 70 ms and bringing in S2 by 10 ms until there was loss of atrial capture. We then brought out S2 by 5 ms until atrial capture returns. This procedure was repeated with a drive cycle 100 ms beginning with an S2 coupled at 70 ms. *Atrial Double Extrastimuli* were delivered to determine atrial arrhythmia inducibility with a train of 8 S1s at a cycle length of 120 ms, an S2 coupled at 70 ms and an S3 coupled at 70 ms. We then brought in S3 by 10 ms until it was just below atrial effective refractory period (AERP) and then brought in S2 by 10 ms until it was below AERP. *Atrial Triple Extrastimuli* were also delivered to determine atrial arrhythmia inducibility with a train of 8 S1s at a cycle length of 120 ms with an S2 coupled at 70 ms, an S3 coupled at 70 ms and an S4 also coupled at 70 ms. We brought in S4 by 10 ms until it was just below AERP and then repeated the protocol as above with atrial doubles. Atrial Burst Pacing**,** to determine atrial arrhythmia inducibility, was delivered as a train of 28 S1s at a cycle length of 50 ms followed by four extrastimuli with a coupling interval of 30 ms for about 20 seconds with a pause of one second in between trains. We then repeated this protocol with a train of 48 S1s for 20 more seconds followed by 20 seconds more with a train of 8 S1s. Retrograde AV Conduction was determined by delivering ventricular pacing at a cycle length of 120 ms and incrementing the pacing cycle length by 10 ms steps until there is 1:1 VA conduction or the paced cycle length exceeded the sinus cycle length. Right Ventricular Effective Refractory Period was determined by delivering a train of 8 S1s at a cycle length of 120 ms with an S2 coupled at 70 ms and bringing in S2 by 10 ms until S2 failed to capture, and then bringing out S2 by 5 ms to find the refractory period. The protocol was repeated at a drive cycle of 120 ms and then 100 ms coupled with an S2 at 70 ms. *Ventricular Double Extrastimuli* were delivered as a train of 8 S1s at a cycle length of 120 ms with an S2 coupled at 70 ms and an S3 coupled at 70 ms. We brought in S3 by 10 ms decrements until it was refractory or down to 50 ms, then we brought in S2 by 10 ms and brought out S3 by 10 ms and continued this stepwise process until S2 was refractory. *Ventricular Triple Extrastimuli* were also delivered as a train of 8 S1s with the same drive cycle as used for the ventricular double extrastimuli with an S2, S3 and S4 coupled at 70 ms each. We repeated the protocol as above for ventricular double extrastimuli starting with S4 and brought in each extrastimuli until it was refractory or down to 50 ms in the same stepwise process until S2 was refractory. Ventricular Burst Pacing to determine ventricular arrhythmia inducibility was delivered as a train of 28 S1s at a cycle length of 50 ms followed by four extrastimuli with a coupling interval of 30 ms for about 20 seconds with a pause of one second in

between trains. We then repeated the protocol with a train of 48 S1s for 20 more seconds followed by 20 seconds more with a train of 8 S1s.

Histology and immunohistochemistry

Detailed protocols used for histological and immunohistochemical staining have been previously described(Ismat et al., 2005; Liu et al., 2008; Levin et al., 2009; Liu et al., 2015). For histological analysis, mice were injected with heparin (100 units IP) and 5 minutes later they were euthanized by pentobarbital overdose (120 mg/kg IP). The hearts were then rapidly excised through a sternotomy, rinsed in ice-cold phosphate-buffered saline (PBS) and fixed in 2% paraformalin in PBS for 12-16 hours. Dogs were euthanized using Euthasol (0.05 mL/kg IV) and the right and left atrium were then harvested through a midline sternotomy, rinsed in ice-cold PBS and fixed in 2% paraformalin in PBS for 12-16 hours. Explanted human hearts were harvested in the operating room after the patient was placed on cardiopulmonary bypass and cardioplegia induced with Visaspan (potassium lactobionate, 100 mM; KH_2PO_4, 25 mM; $MgSO_4$, 5 mM; raffinose, 30 mM; adenosine, 5 mM; glutathione, 3 mM; allopurinol, 1 mM; hydroxyethyl starch, 50 g/L) at 30ºC. Sections of the left and right atrium and ventricles were then quickly dissected apart and rinsed of blood in ice-cold Visaspan and then fixed in 4% paraformalin in PBS plus 24 mM KCI for 16-20 hours. Fixed myocardial tissue from both animals and humans was dehydrated and embedded in paraffin wax according to standard procedures. Sections of fixed tissue were then cut and mounted on slides (4-6 μm), dewaxed in xylene and rehydrated through an ethanol series. For immunohistochemical analysis the slides were heated in 1X Antigen Unmasking Solution (Vector Laboratories) in a 350W microwave oven for 10 minutes to expose the epitope. Fixed sections were washed in PBS before blocking with 5% skim milk in PBS for 30 minutes and then incubated overnight at 4ºC with primary antibodies. The primary antibodies used were a rabbit polyclonal anti-CD19 antibody (1:100, AF1700, R&D Systems); rabbit polyclonal anti-CD4 antibody (1:100, AB119814, AbCam), rabbit polyclonal anti-CD163 antibody (1:100, sc-20066, Santa Cruz); rabbit polyclonal anti-CD68 antibody (1:100, AB6673, AbCam); rabbit polyclonal anti-Perilipin1 (1:100, sc-489, Santa Cruz); rabbit polyclonal anti-Pref1 antibody (1:100, sc-17871, Santa Cruz); rabbit polyclonal anti-TNFα antibody (1:100, AB6673, Santa Cruz); rabbit polyclonal anti-IL-6 antibody (1:100, AB6673, Santa Cruz); rabbit polyclonal anti-leptin antibody (1:100, AB6673, Santa Cruz) or rabbit polyclonal anti-adiponectin antibody (1:100,

AB6673, Santa Cruz) diluted with 5% skim milk in PBS. After washing in PBS, sections were incubated with Alexa488- or Alexa594- conjugated rabbit anti-mouse or goat anti-rabbit secondary antibodies at a 1:500 dilution for 1 hour at room temperature for fluorescent images, or using the secondary antibody provided with a commercially available kit for DAB stained sections (1:200, AB64264, AbCam). Sections were then washed in PBS and mounted for analysis using a Nikon TE200 microscope equipped with a CCD camera and epifluorescence capabilities or a Zeiss LSM 510 confocal microscope.

Statistical analysis

Differences in means among multiple data sets were analyzed using 1- or 2-way ANOVA with treatment or presence of atrial fibrillation as the independent factors. When ANOVA showed significant differences, pairwise comparisons between means were tested using Tukey post-hoc analysis. When data were not normally distributed, ANOVA on ranks was used with the Kruskal-Wallis test, followed by pairwise comparison using the Dunn test. Data sets with smaller sample sizes ($n \leq 5$) were compared using the Wilcoxon rank sum test. All values are reported as the mean ± 1 standard deviation, unless otherwise noted. A probability value < 0.05 was considered significant.

Supplemental References

Ismat FA, Zhang M, Kook H, Huang B, Zhou R, Ferrari VA, Epstein JA and Patel VV (2005) Homeobox protein Hop functions in the adult cardiac conduction system. *Circ Res* **96**:898-903.

Levin MD, Lu MM, Petrenko NB, Hawkins BJ, Gupta TH, Lang D, Buckley PT, Jochems J, Liu F, Spurney CF, Yuan LJ, Jacobson JT, Brown CB, Huang L, Beermann F, Margulies KB, Madesh M, Eberwine JH, Epstein JA and Patel VV (2009) Melanocyte-like cells in the heart and pulmonary veins contribute to atrial arrhythmia triggers. *J Clin Invest* **119**:3420-3436.

Li J, Patel VV, Kostetskii I, Xiong Y, Chu AF, Jacobson JT, Yu C, Morley GE, Molkentin JD and Radice GL (2005) Cardiac-specific loss of N-cadherin leads to alteration in connexins with conduction slowing and arrhythmogenesis. *Circ Res* **97**:474-481.

Liu F, Levin MD, Petrenko NB, Lu MM, Wang T, Yuan LJ, Stout AL, Epstein JA and Patel VV (2008) Histone-deacetylase inhibition reverses atrial arrhythmia inducibility and fibrosis in cardiac hypertrophy independent of angiotensin. *Journal of molecular and cellular cardiology* **45**:715-723.

Liu F, Lu MM, Patel NN, Schillinger KJ, Wang T and Patel VV (2015) GATA-Binding Factor 6 Contributes to Atrioventricular Node Development and Function. *Circulation Cardiovascular genetics* **8**:284-293.

Mitacchione G, Powers JC, Grifoni G, Woitek F, Lam A, Ly L, Settanni F, Makarewich CA, McCormick R, Trovato L, Houser SR, Granata R and Recchia FA (2014) The gut hormone ghrelin partially reverses energy substrate metabolic alterations in the failing heart. *Circulation Heart failure* **7**:643-651.

Woitek F, Zentilin L, Hoffman NE, Powers JC, Ottiger I, Parikh S, Kulczycki AM, Hurst M, Ring N, Wang T, Shaikh F, Gross P, Singh H, Kolpakov MA, Linke A, Houser SR, Rizzo V, Sabri A, Madesh M, Giacca M and Recchia FA (2015) Intracoronary Cytoprotective Gene Therapy: A Study of VEGF-B167 in a Pre-Clinical Animal Model of Dilated Cardiomyopathy. *J Am Coll Cardiol* **66**:139-153.

Yuan L, Wang T, Liu F, Cohen ED and Patel VV (2010) An evaluation of transmitral and pulmonary venous Doppler indices for assessing murine left ventricular diastolic function. *J Am Soc Echocardiogr* **23**:887-897.

ADDITIONAL TABLES AND FIGURES

Supplemental Table 1. Arrhythmia and Echo Data from HopX^{Tg} Mice

	HopX^{Tg} (n=8)	Wildtype (n=8)	CI994-HopX^{Tg} (n=8)	CI994-Wildtype (n=8)
Weight (grams)	24.4 ± 1.8	23.9 ± 2.0	24.7 ± 1.6	24.2 ± 1.4
Age (days)	108 ± 5.5	109 ± 7.0	106 ± 6.3	107 ± 6.8
Heart rate (bpm)	496 ± 46.7	483 ± 44.3	490 ± 42.8	488 ± 45.1
Episodes AT	23*†‡	8§	6§	5§
Duration AT (s)	3.8 ± 1.2*†	0.35 ± 0.24§	0.29 ± 0.17§	0.25 ± 0.19§
AT CL (ms)	42.6 ± 8.4	41.9 ± 7.8	43.5 ± 8.2	44.8 ± 7.6
Mice with AT	7/8*†‡	2/8§	2/8§	2/8§
Episodes VT	4	4	2	2
Duration VT (s)	2.97 ± 1.58	2.76 ± 0.96	1.88	1.79
VT CL (ms)	52.4 ± 8.7	51.5 ± 7.6	52.9 ± 8.1	55.7 ± 7.9
Mice with VT	2/8	2/8	1/8	1/8
LA/BW ratio (mg/g)	0.85 ± 0.09*‡	0.49 ± 0.07†§	0.89 ± 0.11*‡	0.46 ± 0.05†§
LA EDL axis (mm)	2.30 ± 0.33*‡	1.64 ± 0.22†§	2.24 ± 0.29*‡	1.60 ± 0.23†§
LA EDS axis (mm)	2.64 ± 0.30*‡	1.80 ± 0.27†§	2.69 ± 0.34*‡	1.74 ± 0.26†§
LVEF (%)	84.7 ± 11.2*‡	62.2 ± 8.9†§	85.0 ± 10.4*‡	85.0 ± 10.4†§
LV EDP (mmHg)	9.0 ± 1.9*‡	4.7 ± 1.6†§	8.7 ± 2.2*‡	4.5 ± 1.8†§
LV ESP (mmHg)	99 ± 9.7	106 ± 10.4	101 ± 9.2	108 ± 9.6

*P<0.05 vs. Wildtype; †P<0.05 vs. CI994-HopX^{Tg}; ‡P<0.05 vs. CI994-Wildtype; §P<0.05 vs. HopX^{Tg}; AT=atrial tachycardia; VT=ventricular tachycardia, CL=cycle length; LA=left atrium; LV=left ventricle; BW=body weight; EDL=end-diastolic long; EDS=end- diastolic short; EDP=end-diastolic pressure; ESP=end-systolic pressure.

Supplemental Table 2. Clinical Characteristics of Heart Transplant Recipients at Explant

	Non-Failing, Sinus Rhythm (n=3)	Systolic Failure Sinus Rhythm (n=9)	Systolic Failure, Atrial Fibrillation (n=9)
Age (years)	48 ± 14*†	70 ± 7.2‡	72 ± 6.6‡
Weight (lbs)	68 ± 7.4	59 ± 6.5‡	60 ± 6.8‡
Gender (M/F)	2/1*†	6/3‡	5/4‡
BMI (kg/m^2)	22 ± 3.7	18 ± 3.4‡	17 ± 4.0‡
Systolic blood pressure (mmHg)	N/A	91 ± 8.9	88 ± 7.5
Diastolic blood pressure (mmHg)	N/A	62 ± 7.2	60 ± 6.7
Left ventricular ejection fraction (%)	59 ± 5.3*†	8.2 ± 3.1‡	7.8 ± 2.9‡
Left atrial size, long axis (mm)	36 ± 2.7*†	45 ± 3.3‡	48 ± 4.1‡
PA systolic pressure (mmHg)	N/A	39 ± 5.2	43 ± 6.1
Mean PA wedge pressure (mmHg)	N/A	17 ± 4.0	19 ± 4.4
Arterial hypertension	1/3*†	7/9‡	8/9‡
Insulin-dependent diabetes	0/3*†	2/9‡	2/9‡
Noninsulin-dependent diabetes	1/3*†	5/9	6/9
Hyperlipidemia	1/3*†	4/9‡	5/9‡
Cigarette smoking history	1/3*†	2/9‡	2/9‡
Pulmonary hypertension	0/3*†	9/9‡	9/9‡
Internal cardioverter defibrillator	0/3*†	6/9‡	8/9‡
Permanent pacemaker	0/5*†	2/9‡	2/9‡
Ventricular tachycardia	0/3*†	9/9*‡	8/9‡
Ventricular assist device	0/3*†	7/9‡	8/9‡
Beta-blockers	1/3*†	8/9‡	8/9‡
Angiotensin converting enzyme inhibitor	1/3*†	8/9‡	9/9‡
Angiotensin receptor blockers	0/3*†	2/9‡	1/9‡
Calcium channel blockers	0/5*†	1/9‡	2/9‡
Aspirin (%)	2/3*†	8/9‡	8/9‡
Loop diuretics	0/3*†	9/9‡	9/9
Digoxin	0/3*†	4/9‡	5/9‡
Sotolol	0/3*†	0/9‡	2/9‡
Amiodarone	0/3*†	3/9‡	8/9‡

*P<0.05 vs. Systolic failure, sinus rhythm; †P<0.05 vs. Systolic failure, atrial fibrillation; P<0.05 vs. Non-failing, sinus rhythm; PA=pulmonary artery.

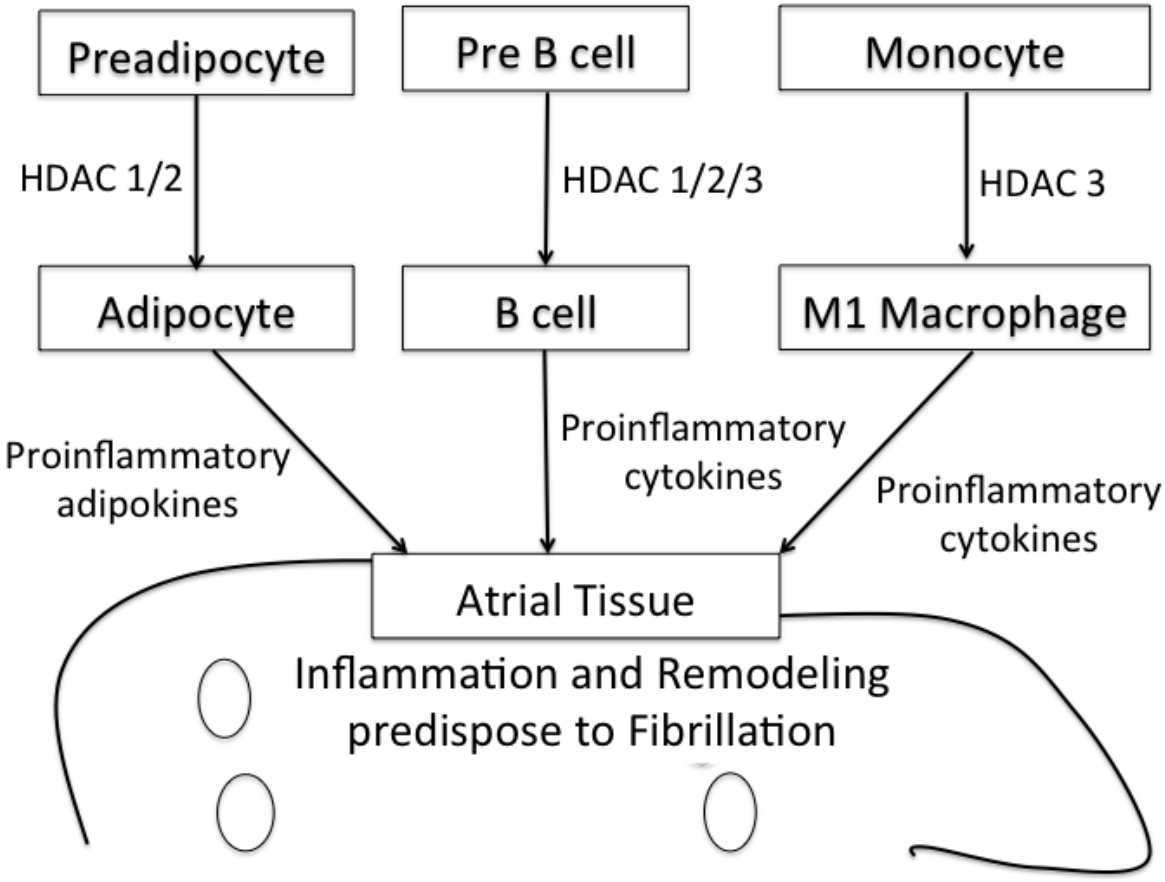

Supplemental Figure 1. Hypothesized involvement of members of class I HDAC in the process of atrial remodeling and inflammation

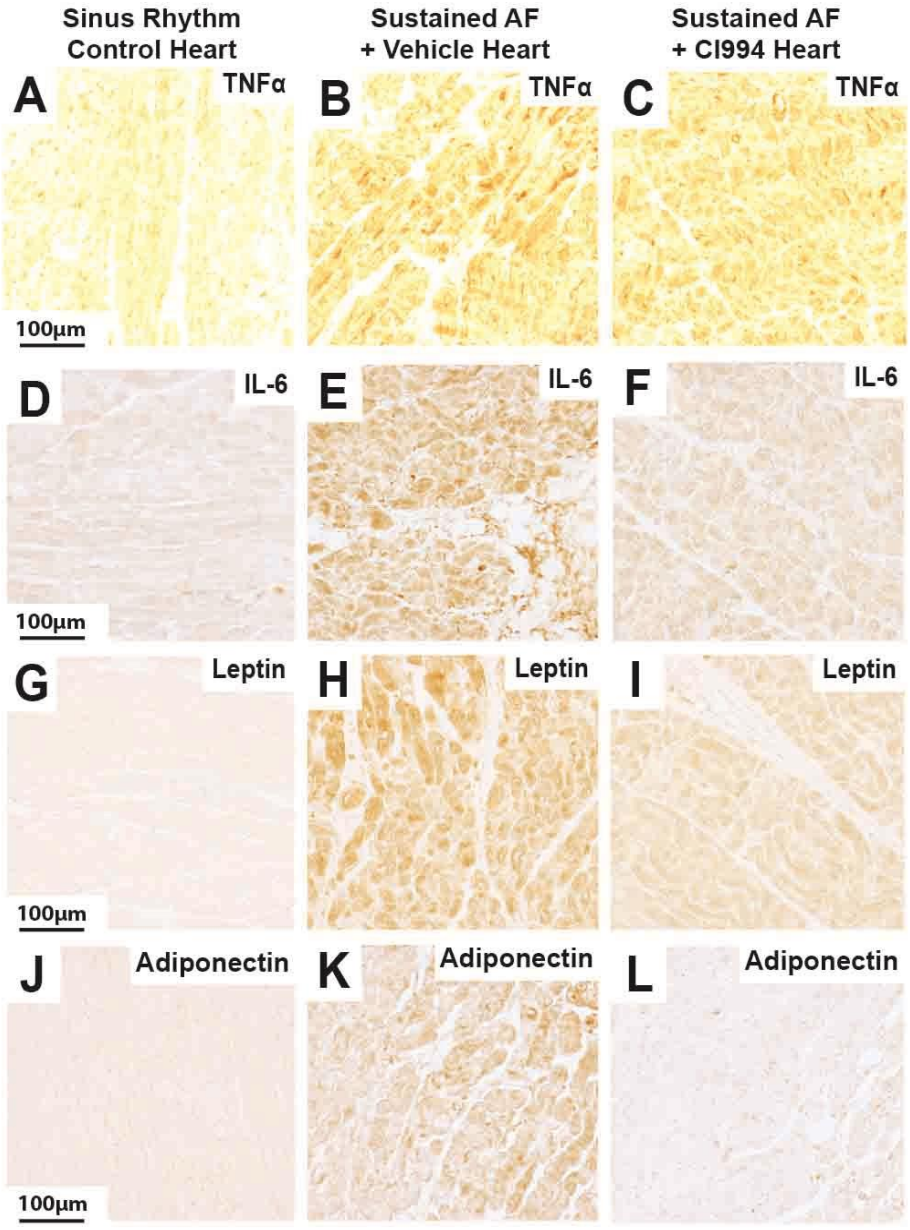

Supplemental Figure 2. *CI-994 reduces atrial cytokine expression in dogs with sustained AF*. Representative images of immunohistochemical staining on canine left atrial sections with antibodies against (A-C) TNFα, (D-F) IL-6, (G-I) leptin and (J-L) adiponectin from (A, D, G and J) control dogs in sinus rhythm, (B, E, H and K) dogs with atrial tachypacing-induced sustained AF and (C, F, I and L) dogs with sustained AF treated with CI-994. Scale bar in left-hand panel applies to that row. Images are representative of 10 different images from 5 hearts/group for each marker.

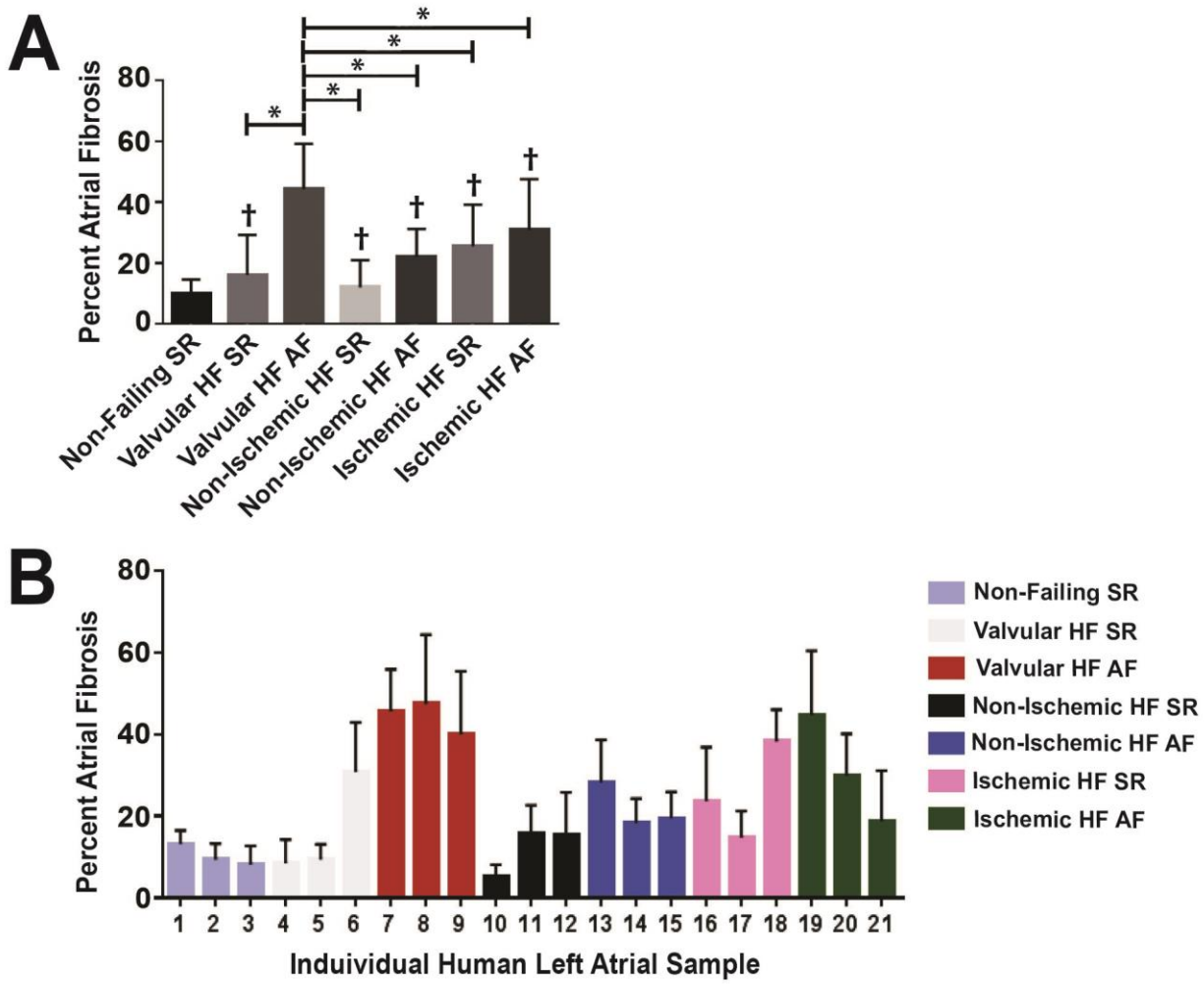

Supplemental Figure 3. *Atrial fibrosis is increased in human left atrium based on heart failure etiology and with atrial fibrillation.* (A) Plot showing the percent fibrosis in left atrial sections excised from explanted failing human hearts due to various etiologies. Note that the highest percent area of fibrosis was observed in atrium from hearts with valvular heart disease (mitral regurgitation) and atrial fibrillation. (B) Plot showing the percent of left atrial fibrosis from each of the human samples analyzed based upon their etiology of heart failure and cardiac rhythm. Although variability exists from sample-to-sample, in general the percent atrial fibrosis is higher when there is atrial fibrillation compared to sinus rhythm for the same etiology of heart failure. At least 20 fields/atrium from 3 different atrium/group were analyzed. $^{*}p<0.01$; $^{\dagger}p<0.05$ vs. Non-failing sinus rhythm (SR); HF=heart failure; SR=sinus rhythm; AF=atrial fibrillation.

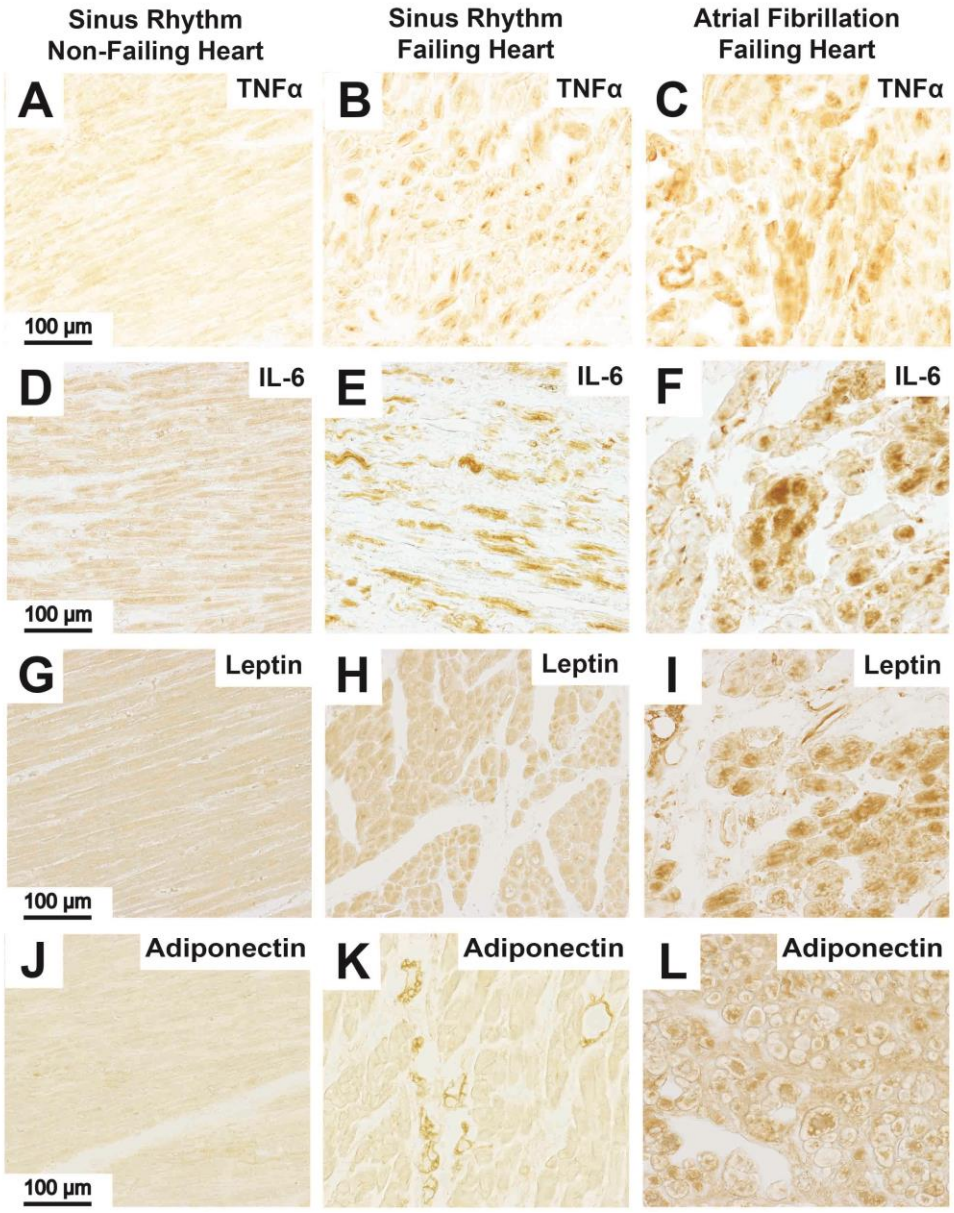

Supplemental Figure 4. *Heart failure and chronic AF increases human atrial cytokine expression.* Representative images of immunohistochemical staining of human left atrial sections with antibodies against (A-C) TNFα, (D-F) IL-6, (G-I) leptin and (J-L) adiponectin from (A, D, G and J) patients in sinus rhythm without heart failure, (B, E, H and K) patients in sinus rhythm with end-stage heart failure and (C, F, I and L) patients with chronic AF and end-stage heart failure. Scale bar in left-hand panel applies to that row. Images are representative of 10 different images from 3 hearts/group for each marker.